Geological Quarterly, 2021, 65: 33
DOI: http://dx.doi.org/10.7306/gq.1603

Unconfined compressive strength of Lower Paleozoic shales from the Baltic Basin (northern Poland)

Michał WOJTOWICZ[1], Marek JAROSIŃSKI[2] and Radomir PACHYTEL[2, *]

[1] Wellfield Geoscience, Grzegórzecka 67C/102, 31-559 Kraków, Poland

[2] Polish Geological Institute – National Research Institute, Rakowiecka 4, 00-975 Warszawa, Poland

Wojtowicz, M., Jarosiński, M., Pachytel, R., 2021. Unconfined compressive strength of Lower Paleozoic shales from the Baltic Basin (northern Poland). Geological Quarterly, 2021, 65: 33, doi: 10.7306/gq.1603

Associate Editor: Beata Jaworska-Szulc

Unconfined compressive strength (UCS) is one of the crucial parameters for geomechanical modelling of unconventional reservoirs useful for the design of hydraulic stimulation of hydrocarbon production. In spite of a large amount of UCS data collected from the Lower Silurian and Ordovician shale successions of the Baltic Basin (northern Poland), no comprehensive study on this subject has been published so far. Here, we compile the results of 247 single-stage confined compressive strength tests (CCST) provided by our industrial partner from four exploration boreholes. Based on the integration of these results with geophysical logging data, including dipole sonic logs, we derive empirical equations describing the relationship between UCS and Young's modulus or sonic wave slowness. Considering the strong anisotropy of elastic properties in shales we have introduced different empirical equations for UCS_V (vertical) and UCS_h (horizontal), respectively perpendicular and parallel to bedding. The formula for UCS_h is determined with less accuracy than for UCS_V due to scarce laboratory tests with bed-parallel loading. Based on the empirical formula proposed, we have estimated the VTI-type of anisotropy to be in the range of 12–27%, depending on the lithostratigraphic formation. The results of our UCS estimations are compared with the results of multi-stage CCST from the adjacent borehole. Both confined tests yielded similar results for $UCS_{V,}$ with slightly higher values obtained from the multi-stage tests. In turn, a comparison of our solution with the results of true uniaxial compressive strength tests (UCST) for vertical samples from one of the studied boreholes revealed a significant discrepancy. The mean UCS results for shale formations from UCST are several times lower than those evaluated from the single-stage CCST. The usefulness of the results obtained for borehole breakout analysis is discussed.

Key words: unconfined compressive strength, triaxial strength tests, empirical equations, shale complexes, Baltic Basin.

INTRODUCTION

Unconfined compressive strength (UCS) together with friction angle (ø), coefficient of internal friction (μ= tan ø), and cohesion (C_0) are basic rock strength parameters commonly used in the Mohr-Coulomb failure criterion (Jaeger and Cook, 1979). UCS is a key factor for geomechanical analysis of shale reservoirs, useful in hydraulic fracturing design and interpretation of its results (Zoback, 2019). In particular, knowing the UCS value is necessary to perform wellbore stability and sand production analyses, constraining *in situ* stress magnitudes from wellbore wall failure, simulation of drilling penetration rate, drill bit wear analysis, and structural modelling of tectonic faulting (Crawford et al., 2010). Our goal was to determine UCS for a future study of stress profiles from the presence of borehole breakouts (Gazaniol et al., 1995; Zoback, 2010), which constitute part of a more complex wellbore stability analysis.

UCS can be simply determined by a direct uniaxial compressive strength test (UCST), conducted without confining pressure. However, these simple tests reduce the most interesting *in situ* UCS values due to the existence of open micro-cracks produced during rock coring, core relaxation, sample preparation, and drying, which is especially important for shale (Josh et al., 2012). These effects cause the rock sample to fail under uniaxial load in one step, providing neither a good measure of the C_0 nor the internal friction angle for the Mohr-Coulomb strength model for reservoir studies (Khaksar et al., 2009). Therefore confined compressive strength tests (CCST), in which technological cracks in a sample are closed under confining pressure, are considered to provide more credible and useful measurements of UCS (King, 1912; Robertson, 1955). Technically, there are two methods for evaluating UCS from the results of CCST on core samples (ISRM, 1983):

– multi-stage CCS testing, in which several measurements are performed on one sample allowing construction of the failure envelope (Kovari et al., 1983);
– single-stage CCST performed on several samples similar in terms of lithological and possibly mechanical properties.

* Corresponding author, e-mail: rpac@pgi.gov.pl

Received: July 6, 2020; accepted: May 13, 2021; first published online: July 7, 2021

In this case, careful sample selection for UCS tests is important, especially for shale in which mechanical properties may change from bed to bed. Considering sample homogeneity, a multi-stage CCST performed on one sample is a better method, more accurate while less time- and cost-consuming due to a lower number of core samples needed. There are also some shortcomings of multi-stage CCST that stem from uncertainties in recognition of initial rock failure due to loading steps, and the fact that each successive stage is performed on a partially failed rock sample (Youna et al., 2010). For the purpose of our study, we had access to the results of single-stage CCST, which were provided by our industrial partner.

There are also some other indirect methods of UCS determination such as a scratch test for fine-scale strength profiling (Suárez-Rivera et al., 2003) and Schmidt hammer for semi-continuous rock mechanical properties (Taylor and Appleby, 2006). In contrast to CCS tests, these are non-destructive and do not require special core preparation, but need calibration with laboratory data.

Mechanical analyses of core samples are usually not available in the large amounts necessary for determination of the UCS differentiation in the highly variable shale profiles of a sedimentary basin. Therefore, a small number of samples allow only their use for calibration of geophysical logs resulting in the construction of the continuous strength profile of a borehole. To optimize log-core calibration many empirical relations have been introduced (overviews in Chang et al., 2006; Mavko et al., 2009). However, there is no single generic empirical relationship that would be suitable for all cases. All relationships are limited to particular rock types, formations, or work only regionally (Crawford, 2010). The most used geophysically derived UCS predictors are Young's modulus (*E*), P-wave velocity (*Vp*), sometimes expressed as slowness (DTP), and formation porosity (Chang et al., 2006). Applicability of empirical relations for regional use comes with the assumption that geomechanical parameters for a particular lithostratigraphic formation do not significantly change at the wide regional scale (Horsrud, 2001; Chang et al., 2006).

Until recently, most of the UCS laboratory measurements for the oil industry in Poland were performed under uniaxial load in a direction perpendicular to bedding planes. In this paper, we analyse the results of CCST under vertical and horizontal compression in order to provide the empirical relations of UCS to anisotropic petrophysical parameters derived from the dipole acoustic tool logging (Wojtowicz and Jarosiński, 2019). Finally, our results are compared to the UCS data derived from the true uniaxial tests, taken on samples from one of the boreholes studied, and to the data from multi-stage CCST from the borehole adjacent to the study area. One of the main aims of this contribution is to demonstrate the quality and quantity of data available from the Baltic Basin and show an example of their synthesis. Such an analysis is a necessary step on the way to recognizing the state of contemporary stresses in the basin from borehole wall failure, which we also referred to in the discussion.

GEOLOGICAL SETTING

Our study area is located within the early Paleozoic Baltic Basin in northern Poland (Fig. 1). The Ordovician and lower Silurian shale successions analysed accumulated in the calm sedimentary environment of the distal part of the Caledonian foredeep basin (Poprawa et al., 1999; Poprawa, 2019); therefore, the facies are laterally relatively homogeneous at a basin-scale (Pachytel et al., 2017). That allows us to group the samples taken from four boreholes, located 70 km apart, into similar classes related to lithofacies.

Data used in the study are provided by the Polish Oil and Gas Co. from four shale gas exploration boreholes (Fig. 1A). Geomechanical analyses were performed at the Department of Geomechanics of the University of Warsaw (confined CCST) and at the Department of Geomechanics, Civil Engineering and Geotechnics of AGH (unconfined UCST). For the purpose of this work, the boreholes are called B-1, B-2, B-3, and B-4. The borehole core samples and logs analysed were taken from the relatively homogeneous, flat-lying early Paleozoic shale successions without significant internal tectonic deformation. Among the formations analysed, the Piaśnica, Sasino, and Jantar dark shales are considered as gas prospects (Fig. 1B). The Prabuty and Kopalino formations, which separate the most promising units, are highly enriched in carbonate. The uppermost of the units analysed units, the Pelplin Formation, is a bright shale with a total organic carbon content of <1%.

THEORETICAL BACKGROUND

Let us consider a cylindrical rock sample (Fig. 2A) with applied axial σ_1 and confining σ_3 stresses. At a given σ_3, the σ_1 is increased until the rock undergoes irreversible deformation. The value of σ_1 at this point is called the rock strength or peak strength which, apart from the internal properties of the rock, depends also on the applied confining stress σ_3. Rock strength can be described in terms of the Mohr-Coulomb failure criterion, graphically represented by the Mohr failure envelope (Fig. 2B). Semicircles constructed using a set of stress pairs (σ_1, σ_3) at which rock fails, define the envelope line. The UCS is an amount of σ_1 for which $\sigma_3 = 0$; therefore, it is also called the uniaxial compressive strength. The simple failure criterion describing the linear failure envelope is as follows (Jaeger and Cook, 1979):

$$\tau = \mu\sigma_n + S_o \quad [1]$$

where: μ represents the coefficient of internal friction and S_o is cohesion.

The Mohr-Coulomb strength envelope could be also presented in a σ_1/σ_3 coordinate system (Fig. 2C), in which the UCS value is illustrated by the point at which the envelope crosses the σ_1 axis. In this case, the failure criterion is:

$$\sigma_1 = n\sigma_3 + \text{UCS} \quad [2]$$

To fully describe the strength of a rock, apart from UCS, we need to know the slope of an envelope given by n, μ, or the angle of internal friction ø. Relations between these parameters are:

$$\alpha = \frac{\varnothing}{2} + \frac{\pi}{4} \quad [3]$$

$$ø = \arctan(\mu) \quad [4]$$

$$n = \frac{1+\sin(\varnothing)}{1-\sin(\varnothing)} \quad [5]$$

$$\varnothing = \arctan\left(\frac{n-1}{2\sqrt{n}}\right) \quad [6]$$

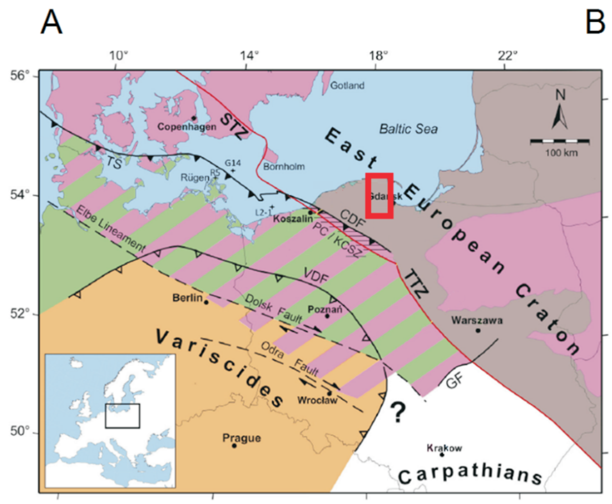

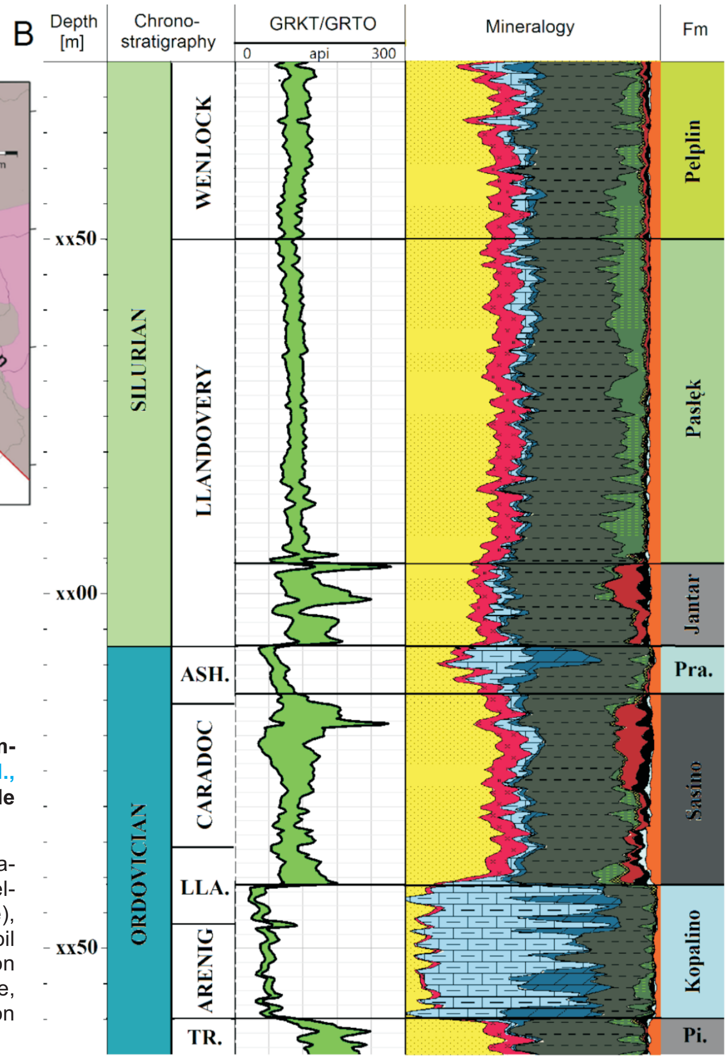

Fig. 1A – location of the boreholes analysed within a simplified tectonic context of Central Europe (Mazur et al., 2015); B – the stratigraphic column covered by borehole data

ASH. – Ashgil, LLA. – Llanvirn, TR. – Tremadoc, Pi. – Piaśnica, Pra. – Prabuty; in the mineralogical column: quartz (yellow), feldspar (red), calcite (light blue), dolomite (dark blue), illite (dark green), chlorite (light green), kerogen (reddish), oil (black), bound water (orange); CDF – Caledonian deformation front, GF – Grójec Fault, STZ – Sorgenfrei-Tornquist Zone, TTZ – Teisseyre-Tornquist Zone, VDF – Variscan deformation front

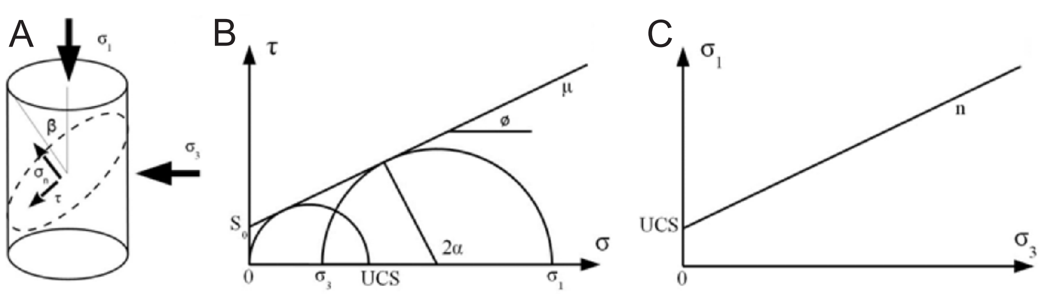

Fig. 2A – a test plug subjected to loads with a plane of failure; B – simplified Mohr linear failure envelope referred to as Mohr-Coulomb failure with a graphic representation of the parameters analysed; C – the Unconfined Compressive Strength (UCS) representation based on Mohr-Coulomb linear failure criteria

Symbols are explained, and the equations are given, in the text

The easiest way to measure UCS is to perform a uniaxial compressive strength test (UCST) under zero confining pressure ($\sigma_3 = 0$), but both the tendency of unconfined rock to split vertically and the presence of micro-cracks induced by core handling (Handwerger et al., 2011) cause the results of such measurements to be clearly lower then UCS determined from confined tests. The discrepancy between the UCS values obtained from uniaxial and triaxial tests is also considered in the Discussion section.

To obtain the UCS value from the single-stage CCST results we had to find the strength envelope of the Mohr-Coulomb diagram. In our simplified approach, forced by the data quality with a minor spread of loading conditions and single-stage tests, only the linear strength envelope could be considered. In order to find the trend of the envelope, one has to group the CCST results performed under different confining pressures into similar groups. Then, for each group, the linear failure envelope was constructed that allows the calculation of UCS and ø (Fig. 2), according to Eq. [2] and [6]. Ideally, all measurements for each failure envelope should be performed on the samples from one uniform bed but in real borehole conditions, where the volume of rock is limited, this is unheard of.

In the previous study (Wojtowicz and Jarosiński, 2019) we have demonstrated that changes in elastic properties of the shale successions studied are homogeneous and exhibit strong anisotropy described as vertical transverse isotropy (VTI). Anisotropy of shales also applies to UCS (Crawford et al., 2012) which means, that UCS perpendicular to bedding (UCS_v) and UCS parallel to bedding (UCS_h) do not have to be equal. Therefore a separation between these measurements has to be made. From the geomechanical point of view, both horizontal and vertical UCS values are useful for application to the shale reservoir (see Discussion section). However, the minimum UCS values in shales are determined in plugs directed obliquely to bedding where the weak lamination planes are sheared (Crawford et al., 2012; Bonnelye et al., 2016). The UCS anisotropy is expressed by strength changes in relation to angle (β) (Fig. 3A) between axial stress σ_1 and bedding planes of the rock (Crawford et al., 2012). According to the above study, the minimum UCS for shale occurs when angle β is in the range of 45–60° (Fig. 3B), and its value could be 20 up to 80% lower than maximum UCS depending on rock type. These values are obtained in the UCS laboratory test or in direct shear tests. Having no access to such data, we have limited our study to the horizontal/vertical UCS anisotropy. That seems to be more suitable for stress analysis in vertical exploration boreholes, in which lamination is orthogonal to the principal stress axis and, therefore, at these planes, the shear stresses are close to 0. For inclined borehole intervals, the lamination may play an important role as a weakening plane influencing borehole wall failure.

DATA FROM THE SINGLE-STAGE CONFINED COMPRESSIVE STRENGTH TESTS

Data from confined compressive strength tests (CCST) were available for all boreholes studied. No multi-stage CCST was performed for any of them. For all boreholes, we possessed 224 single-stage CCST results measured perpendicular to bedding planes, and 25 CCST measured parallel to bedding plane for three boreholes (not for B-1). The CCST tests were performed at the temperature evaluated for the shale reservoir that is variable in a range of 60–90°C. All samples oriented parallel to bedding planes had a nominal diameter of 37 mm and a height twice that. The samples perpendicular to bedding planes had diameters of either 37 or 50 mm and heights twice that. Available data, presented as pairs of σ_1 (peak axial stress) and σ_3 (confining stress) are shown in Figure 4 for each borehole separately. Samples perpendicular to bedding, called vertical (giving UCS_v) are shown separately from samples parallel to bedding, called horizontal (giving UCS_h). The location of samples was chosen by the concession owner to represent formations of interest with more or less constant spacing. The important limitation was that samples parallel to bedding planes were measured under a constant confining pressure of 50 MPa, which is close to the effective lithostatic pressure at the depth of the successions analysed.

UNCONFINED COMPRESSIVE STRENGTH DETERMINATION

A large number of available vertical samples enables us to cluster them in groups for which the USC_v values were possible to determine by means of simple linear inversion using Mohr-Coulomb failure criteria (see Fig. 2C). For the purpose of sample grouping we assumed the following criteria:
- samples should come from the same lithostratigraphic formation,
- samples should have similar lithological features,
- samples should have similar corresponding geophysical log responses,
- separation of samples should be no longer than 25 m,
- samples should be determined from at least two different confining pressures, which is than that recommended by the ISRM (1983), of at least 3 samples.

We have accepted such a solution due to the scarcity of horizontal samples. Following the above assumptions, we were able to distinguish 34 groups of vertical samples. Among these, there are 22 groups having three or more measurements, performed under three or more confining pressures, which provided the most credible control on UCS_v. Another 5 groups have three or more measurements performed under two confining pressures, and the rest consists of only 2 measurements each. In the grouping procedure we have rejected 10 samples (4%) as evident outliers, not meeting the above criteria, and thus obtained 6.1 measurements per group. In the following part of the study, the mean USC_v values for these groups are referred to as the UCS data points in order to differentiate them from the results of individual measurements.

The failure envelope was evaluated for each group using the linear Mohr-Coulomb criteria. UCS_v and ø were calculated using Eq. [2] and [6]. Figure 5 shows two examples of groups while evaluating UCS_v and $ø_v$ in borehole B-1. The depth at which the calculated UCS_v values are marked as data points was set as an average depth of samples assigned to the specific group. To show how our UCS_v estimations fit the data we show the distribution of the coefficient of determination (R^2) for the groups having more than two points (Fig. 6A). For obvious reasons, those groups with two points were not considered in these statistics because

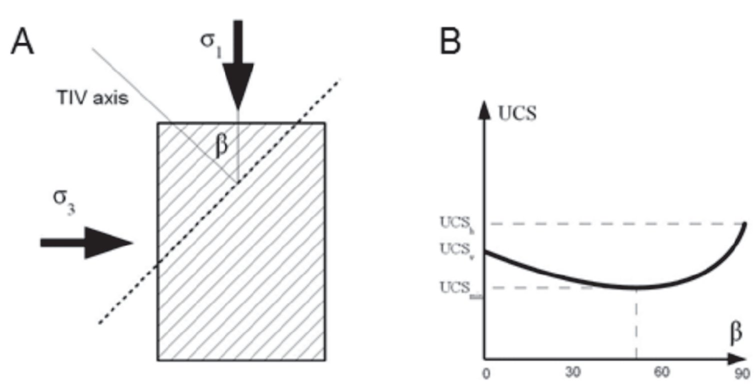

Fig. 3A – core sample cut oblique to VTI axis (and lamination) subjected to triaxial load; B – example of the relation between the UCS value and the angle between axial stress and VTI axis

The minimum UCS under ~50° and the strength anisotropy parallel and transverse to lamination are shown their fit to the line is always perfect. With the proviso that the amount of our data is limited, we can see that for only one UCS_v determination is the coefficient R^2 <0.5. The vast majority of coefficients of UCS_v determination fall into a range of R^2 >0.8. In order to evaluate whether the strength envelopes obtained are acceptable for shales, we show the distribution of internal friction angles ($ø_v$) for the UCS_v data points (Fig. 6B). Except for three outliers, the rest of the $ø_v$ values fall into a broad range of 10–35°, while the mean value of friction angle for all data points is $ø_v$ = 22°. The distribution is not very far from Gaussian. Considering that a compilation for shale reservoirs in the USA reveals ø in the range of 20–38° (Kohli and Zoback, 2013), our results seem reasonable. A graphical representation of the UCS_v values (Fig. 6C) shows their range from 60 to 160 MPa, with a weakly visible trend of Gaussian distribution. One of the reasons for the abnormal UCS_v distribution is the small number of groups. Despite this, the most frequent values are in the middle of this range, between 80–140 MPa.

Bedding-parallel samples were grouped according to similar principles as for the UCS_v, except the last term, which is not applicable due to the constant confining pressure used during testing. To determine the USC_h for such groups we had to make an additional assumption evaluating the slope of the failure envelope. Laboratory studies of fine-grained rocks (Crawford et al., 2012) at various confining pressures, up to 35 MPa, indicate that the angle of internal friction for samples loaded perpendicular to bedding can be either higher or lower than parallel to bedding with a slight predominance of the latter. For determination of the UCS_h we adopted the uniform value of $ø_h$ = 25°, which is typical for shales (Kohli and Zoback, 2013), and only slightly higher than the mean calculated by us for UCS_v data points. In that case, the only unknown in Eq. [2] is UCS_h.

Finally, we obtained 11 UCS_h data points for 3 boreholes that are 2.3 CCST tests for one UCS_h data point on average. Most of the groups were composed of only 2 samples. In this case, the scarce CCST results in groups have no negative impact on UCS_h determination because they could be determined for every single measurement when the $ø_h$ trend is assumed. The distribution of the CCS_h values for samples under constant 50 MPa confining pressure seems to follow a Gaussian trend (Fig. 7A). The most common values fall in between 220–300 MPa. To demonstrate the quality of grouping we show the mean deviation of CCS_h values from the average for each group (Fig. 7B). From the mean deviation of <20 MPa, we can judge that in 7 groups the samples are similar. The rest of the groups are more heterogeneous. Obviously, the identical distribution is for the individual UCS_h values for samples. The distribution obtained of the UCS_h for groups (Fig. 7C) represents values in a range of 90–170 MPa, with a majority >130 MPa.

UCS EMPIRICAL EQUATIONS

There are many UCS estimators that could be used depending on the area of interest, formation, and available data. The most used predictors for UCS are log-derived Young's modulus (*E*) calibrated with laboratory tests, P-wave velocity (*Vp*), sometimes expressed by slowness (DTP), and formation porosity (Chang et al., 2006). Using log-derived parameters is justified by the simplicity of application for other boreholes in the region or basin. The situation is more complicated for anisotropic vertical transverse isotropy (VTI) formations when UCS is not uniform in all directions so the logs do not carry all the information necessary to describe the mechanical properties of the formations. The quality of our data does not allow the full description of UCS value in relation to bedding planes as a function of angle β. However, the data allow consideration of empirical equations for UCS in vertical and horizontal directions. These two directions are especially important for the description of the VTI formations, and UCS_h or UCS_v will be more appropriate to use in failure criteria (Eq. 2) when performing breakout presence predictions.

We had an access to all Young's modulus data measured on samples both perpendicular and parallel to bedding, as well as to raw log datasets containing P-wave slowness, S-wave slowness, and density. Calculated values of perpendicular and parallel Young's modulus (*E*) look like the best predictors of UCS since they were determined based on a full stiffness tensor from the dipole sonic and density logs calibrated with the results of laboratory tests (Wojtowicz and Jarosiński, 2019). The laboratory tests for *E* calibration were the same single-stage CCST tests on horizontal and vertical samples as for the present UCS study. There is no simple dependence between *E* and USC, although they both carry some important information on formation anisotropy (Wilczyński et al., 2021).

Looking for the empirical equation which fits best to laboratory data one may realize that the data available to us are not sufficient to characterize the non-linear function of UCS dependent on *E*. For this relation, we have adopted the form of exponential function $UCS = a \cdot E^b$, which is recommended for shales (compilation in Sone and Zoback, 2013a; Zoback, 2019). The *a* and *b* parameters of this function were determined by matching our data points estimated from laboratory tests to the calculated values (Fig. 8) using the least squares method. Compiling data from all 4 boreholes, we found the best fit for UCS_v and USC_h (Fig. 8), receiving empirical equations (E_v and E_h in GPa while UCS_v and USC_h in MPa):

$$UCS_V = 15.82 \cdot E_{vstat}^{0.61} \quad [7]$$

$$UCS_h = 4.47 \cdot E_{hstat}^{0.91} \quad [8]$$

For these equations, low coefficients of determination R^2 = 0.5 and R^2 = 0.1 for the UCS_v and USC_h respectively indicate that the data are obviously not sufficient to perform a nonlinear regression.

To use the above formula based on borehole logging data the dynamic Young's modulus is necessary. We have adopted the common assumption of a linear relation between static (E_{stat}) and dynamic (E_{dyn}) Young's modulus (Mavko et al., 2009). Then, the E_{stat} measured in laboratory tests on the same samples for which the UCS was examined in both the vertical and horizontal directions, were provided by our industrial partner. In our previous work (Wojtowicz and Jarosiński, 2019), these data were compiled on cross-plots with E_{dyn} derived from the dipole acoustic logging tool. Based on this compilation the best-fitted formulae were derived by applying a least squares method:

$$E_{vstat} = 0.73 \cdot E_{vdyn} - 2.75 \quad [9]$$

$$E_{hstat} = 0.88 \cdot E_{vdyn} - 3.3 \quad [10]$$

It is not common to possess such data from poorly recognized basins at the beginning stage of exploration. Therefore, we have also searched for empirical equations based on P-wave slowness log measurements (DTP), widely available even for older logs, and usually covering long intervals. DTP, however, does not carry information about formation aniso-

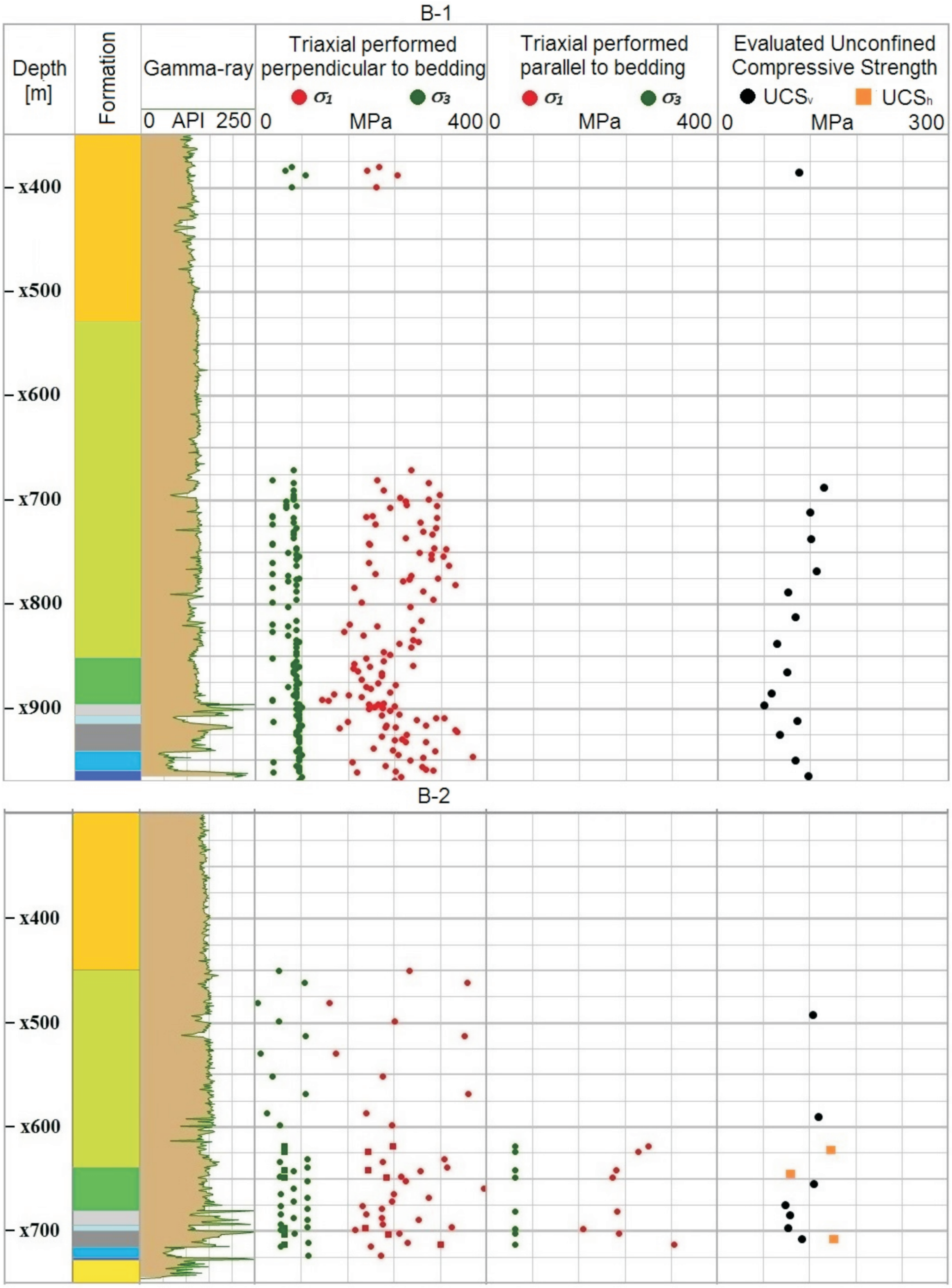

tropy, ther

Fig. 4. Available data from confined compressive strength

Lithostratigraphic formations from the top to the bottom: Kociewie (orange), Pelplin (light green), Pasłęk (dark green),

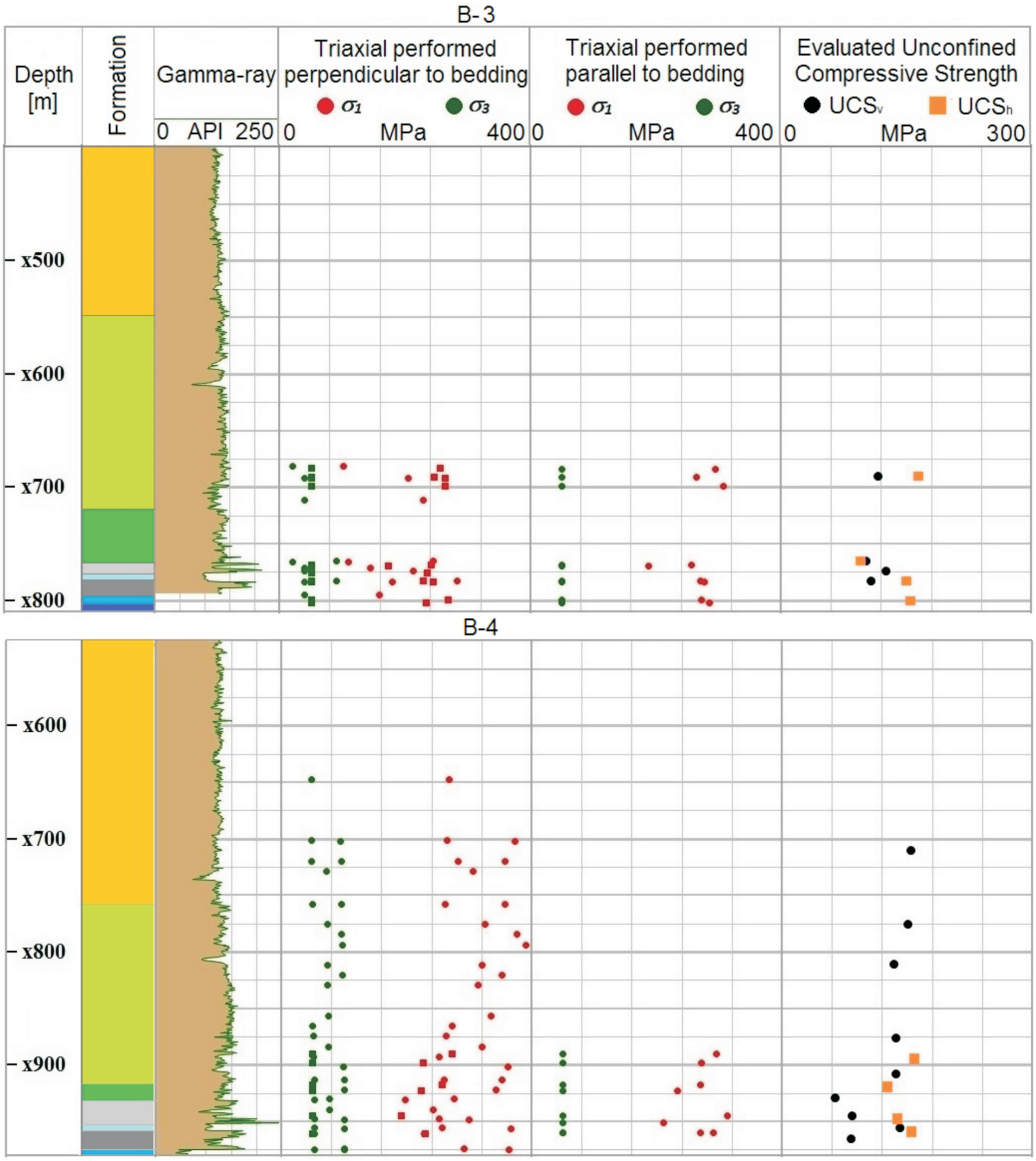

tests (CCST) and UCS values evaluated for the data points

Jantar (light grey), Prabuty (light blue), Sasino (dark grey), Kopalino (blue), Piaśnica (navy blue), Cambrian deposits (yellow)

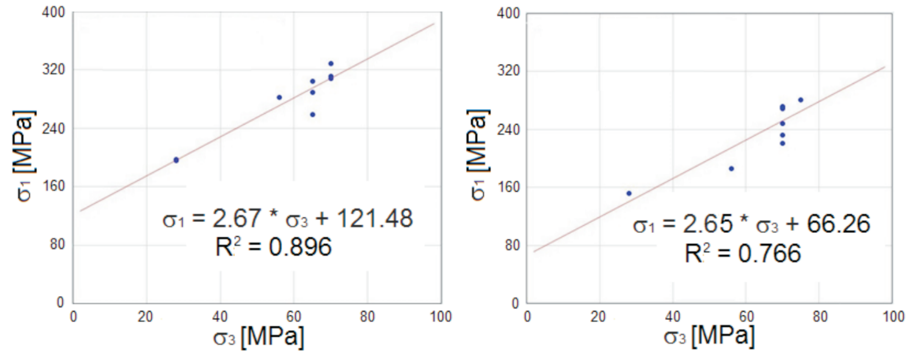

Fig. 5. Examples of constructing a failure envelope based on the data points for UCSv for the B-1 borehole

A – UCS_v 95% confidence intervals 109–134 MPa;
B – UCS_v 95% confidence intervals 45–82 MPa

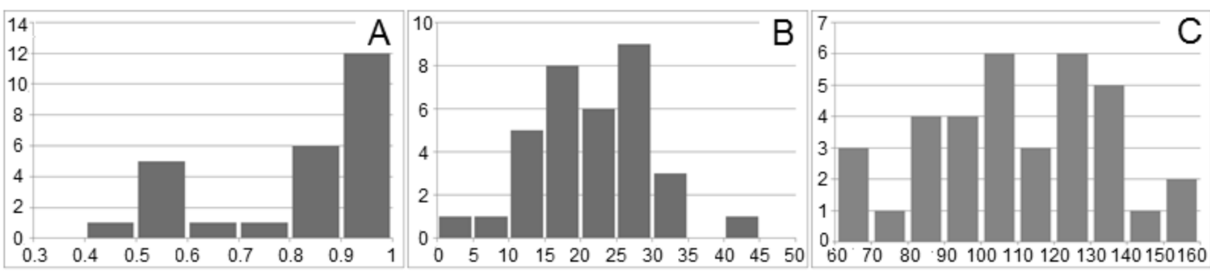

Fig. 6. The results of sample grouping for the UCS_v

A – distribution of coefficients of UCS_v determination (R^2) for groups of samples with more than 2 measurements; **B** – distribution of angles of internal friction ($ø_v$); **C** – distribution of the UCS_v values for groups in MPa

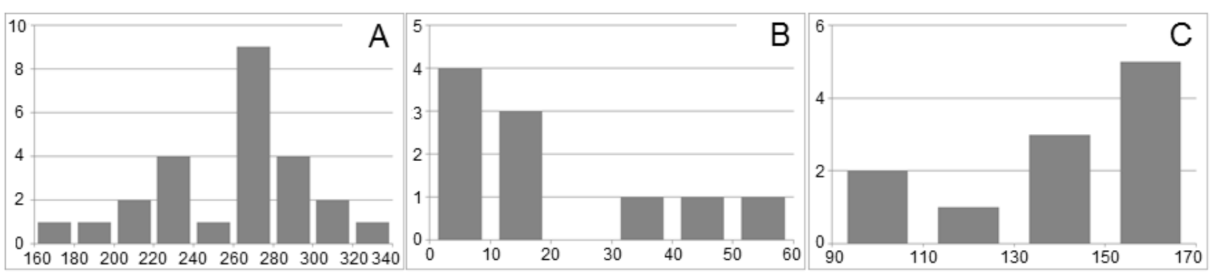

Fig. 7. The results of sample grouping for the UCS_h

A – distribution of UCS_h values for samples loaded in a horizontal direction; **B** – distribution of standard deviation for groups of samples in MPa; **C** – distribution of the UCS_h values for groups in MPa

tropy, therefore it could be used only as a first quick and simple estimator of UCS. For DTP [us/m] we found the following empirical relations:

$$UCS_v = 2.93 \cdot 10^5 \cdot DTP^{-1.85} \quad [11]$$

$$UCS_h = 0.95 \cdot 10^5 \cdot DTP^{-1.51} \quad [12]$$

The determination coefficients are very low, $R^2 = 0.37$ and $R^2 = 0.1$ for the UCS_v and USC_h respectively. Without additional assumptions about the form of this function, it is impossible to derive them through direct regression. Therefore we can conclude that these equations are not strictly determined by the data points, though the constants of the predefined equations are optimized using data.

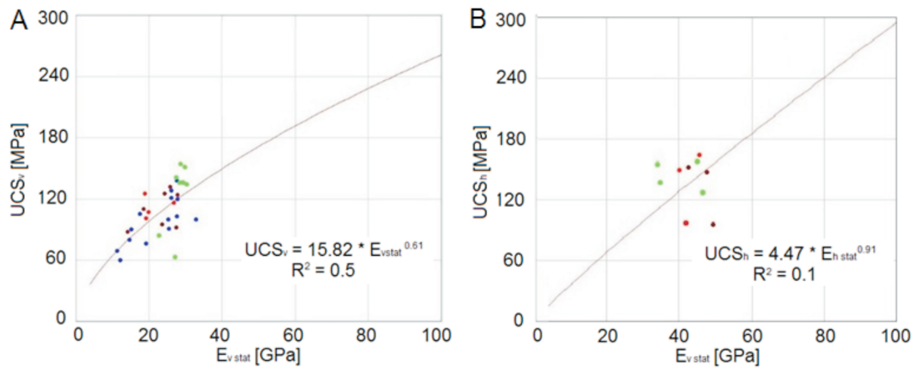

Fig. 8. UCS *versus* static Young's Modulus for data points in both directions

A – vertical; **B** – horizontal; by colour of dots, the shale formations are distinguished; grey bars indicate 95% confidence intervals

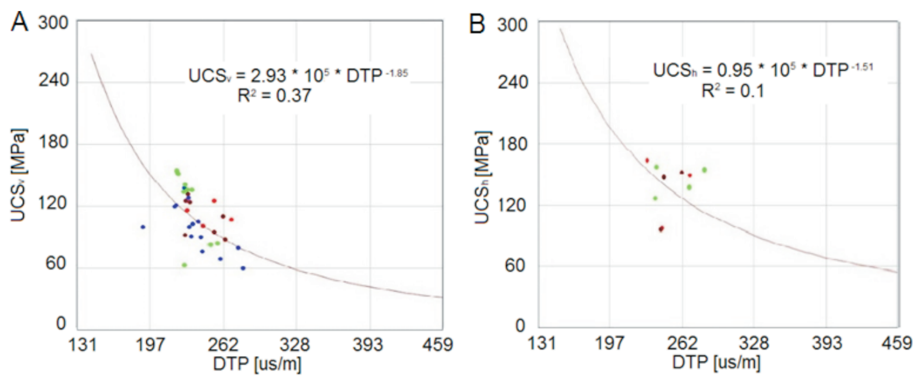

Fig. 9. UCS *versus* DTP for data points in two directions

For explanations see Figure 8

Considering the poor constraint afforded by the empirical equations above, we have checked how the UCS data points deviate from the theoretical values. UCS profiles are shown for four boreholes, correlated with data points (see Fig. 10). From a practitioner's point of view, the visually assessed fit of the calculated UCS values to laboratory measurements using Eq. 9–12 seems acceptable. To quantify the fit of our models to data points we have calculated the standard deviation between the curves and the data points (for Figs. 8–10), summarized for four boreholes. For 34 UCS_v data points, we have obtained a standard deviation of ±18.2 MPa for E_v and ±21.6 MPa for DTP_v estimators. For 11 UCS_h data points, the standard deviation is ±29.3 MPa for E_h and ±27.7 MPa for DTP_h estimators. Significantly better accuracy has been achieved for UCS_v. To determine how significant these standard deviation values are, they have been compared to the UCS values. The UCS for the data points ranges from 60 to 170 MPa with the mean UCS_v = 108.5 MPa and mean UCS_h = 137.8 MPa. Since the standard deviation is ~17% of the mean UCS_v and 20% of the UCS_h, such approximations have to be used with caution.

COMPARISON WITH OTHER UCS DATA FROM THE BALTIC BASIN: A DISCUSSION

The UCS analysis described, for a significant amount of data from four boreholes, shows that the measurements so far have not been optimized for the analysis of useful rock strength. The empirical relations obtained hold a relatively high level of uncertainty. Due to the limited number of the available samples and their clustering at a constant confining pressure, the UCS_h function is matched to data with a significantly higher uncertainty level than the UCS_v. This is a serious drawback, as UCS_h is more important for stress analysis based on borehole breakout data from vertical boreholes. However, it was the best that we could do with the available dataset.

To independently check our results, we have compared them to other sets of data from the same shale basin. For this purpose, we have calculated the mean UCS values for shale formations from the B-1 borehole (Table 1), for which we had an independent set of measurements. Our UCS values were obtained from individual geophysical records (see the number of samples in Table 1) by applying empirical equations for the Young's modulus in vertical and horizontal directions (Eq. 7–10). The mean values of UCS_v for shale formations (Pelplin, Pasłęk Jantar, Sasino, and Słuchowo formations) vary from 83 to 121 MPa, while UCS_h is higher in each case, with values ranging from 108 to 137 MPa. Such results indicate a UCS VTI-type of anisotropy in the range of 12–27%. Slightly higher mean UCS values and lower anisotropy are obtained for marls (Prabuty Formation – 13%) and limestones (Kopalino Formation – 9%). This relationship can be explained by higher carbonate contents at the expense of clay minerals (see Fig. 1) leading to rock matrix lithification with carbonate, which commonly decreases shale anisotropy (Sone and Zoback, 2013b; Guo et al., 2014). The measure of the UCS diversity is given by standard deviation (SD), which varies in a narrow range for lithostrati-

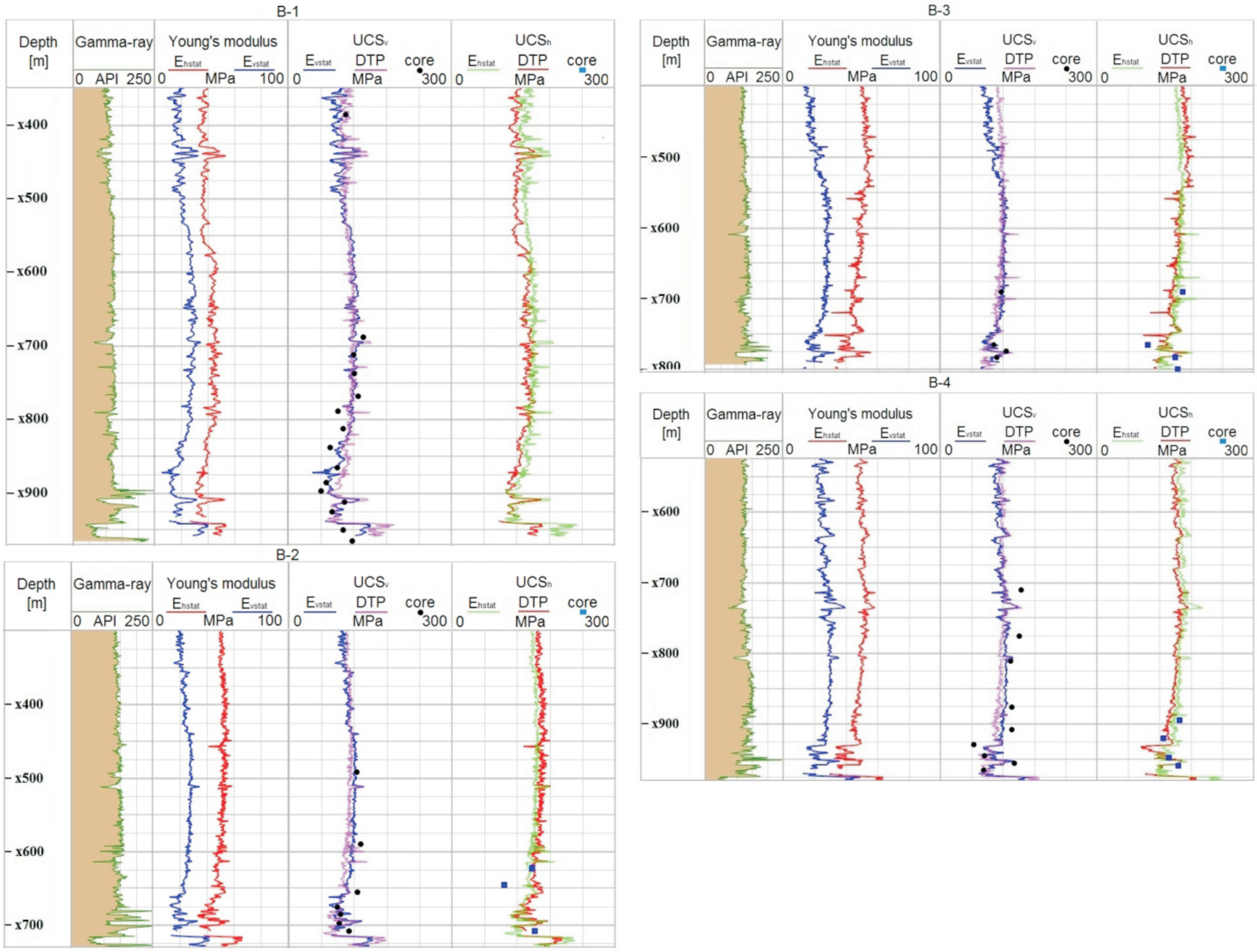

Fig. 10. UCS profiles for the boreholes analysed

Track 5 – data points *versus* calculated empirical UCS_v values, track 6 – data points *versus* calculated empirical UCS_h values

Table 1

Comparison between UCS values obtained for the same shale successions in UCST (for the B-1 borehole), multi-stage CCST (borehole outside the study area), and our results for the B-1 borehole extrapolated through geophysical logs

Formation (shale in bold)	UCST for B-1			Multi-stage CCST for T-1 (7–14 MPa of confining pres.)		Our results for B-1 from geophysical logs using our empirical equations			Anisotropy $(UCS_h–UCS_v)/UCS_h$
	No of sampl.	UCS_v [MPa]	Max. spread of UCS_v [MPa]	No of samples	UCS_v [MPa]	No of samples*	UCS_v ±SD [MPa]	UCS_h ±SD [MPa]	for B-1
Pelplin	41	**45**	(20–87)			3000	**121 ±08**	137 ±08	12%
Pasłęk	4	**22**	(11–38)			458	**85 ±12**	113 ±11	25%
Jantar	2	**15**	(10–21)	2	**103**	116	**83 ± 08**	108 ±06	23%
Prabuty	1	8		1	135	68	122 ±10	140 ±16	13%
Sasino	3	**30**	(8–72)	6	**141**	203	**93 ±06**	110 ±07	16%
Kopalino	2	35		1	126	170	140 ±12	153 ±08	9%
Słuchowo	1	**42**		2	**106**	77	**91 ±32**	125 ±21	27%

The results are for samples loaded in a direction perpendicular to bedding, except for our ones, where those also parallel to bedding are shown; the mean values for shale formations are in bold; the remaining two formations comprise limestone and marl; * – the large number of samples is due to the acceptance of geophysical records as samples graphic formations, below <±16 MPa (except for the Słuchowo Formation where SD = ±32 MPa), pointing to relatively stable UCS values in formations.

The above-determined mean UCS values for formations have been verified by comparison with the results of uniaxial compressive strength tests (UCST) from the same B-1 borehole, and multi-stage confined compressive strength tests (CCST) performed by the industry on samples taken from T-1 borehole, located 15 km away from the study area. The UCST were performed only in a vertical direction. The samples from the shale formations in our study are scarce, except for the Pelplin Formation where 41 tests were performed. The individual UCS_V values vary from 8 to 87 MPa, and the mean values for formations range from 15 to 45 MPa (Table 1). For individual formations, the differences are 6 to 10 times higher than the standard deviation of our results (except for the Słuchowo Formation where it reaches only 1.5 times the standard deviation). Such a significant discrepancy of the UCS_V obtained by different methods from the same borehole intervals needs explanation. Significantly lower strengths from UCST than from confining tests have been described in the literature (e.g., Khaksar et al., 2009) and explained by easier propagation of tectonic and technological cracks, which are open in the UCST tests without confining pressure. The rock in the reservoir lacks a large population of technologically-produced cracks due to core drilling, its extraction to the surface, drying, and cutting the test plugs. These problems are acute in shales with high amounts of clay minerals and fine lamination, which are prone to disintegration while drying or unloading. This is the reason why, for the reservoir studies, the UCS values from CCST tests are preferred above the UCST values.

Finally, we have compared our results with the dataset from the T-1 borehole where multi-stage CCST in a vertical direction were conducted. In the multi-stage tests, every single sample is subjected to several cycles of loading close to, but not reaching, complete failure. Therefore, in each successive stage, the rock may lose strength due to the failure accumulation that may result in flattening of the strength envelope and a decrease in the internal friction angle. To minimize this effect, we have taken two first stages for our estimation of the UCS that were performed under the confining pressures of 7 and 14 MPa. This pressure level is large enough to close the cracks but, at the same time, low enough to prevent a large error caused by extrapolation of the results of measurements with a linear trend to 0 MPa in unconfined conditions. Although the data are scarce, the results are consistent (Table 1). The mean UCS_V values for formations range from 103 to 141 MPa, which is slightly higher than the USC_V obtained by the mean of our equations. This may be astonishing because the scope of confining pressure in multi-stage tests was lower than in the single-stage CCST (20–90 MPa) used for calibration of our equations. Due to a common convex-upwards shape of the Mohr-Coulomb failure envelope, the USC for lower confining pressure is usually lower. We can expect that this discrepancy may result from the difference in sample size, which for the single-stage tests was 1.5–2.0 inches of sample diameter while for the multi-stage only 1 inch, with the same aspect ratio for both.

In the T-1 borehole, horizontal single-stage CCST were also performed at the same laboratory and with the sample size as for the vertical samples from the T-1 borehole, under 21 MPa of confining pressure. Comparison of these results with the CCST in vertical orientation for the samples from the same beds (depth difference in centimetres) and the same confining pressure indicates that for 75% of samples which reveal anisotropy, the horizontal strength was higher than the vertical one, a relation which generally conforms to our results for the B-1 borehole.

From the above comparisons, it is clear that our results are much closer to the multi-stage CCST results than to the UCST measurements. Since a large span of UCS values for shale, ranging between 2–200 MPa, is common in the literature (compiled by Chang et al., 2006), it can be contested as to which results should be used for geomechanical studies. For a technologically intact reservoir, it seems obvious that the UCS values obtained in CCST are appropriate. However, it can be questioned as to which values should be used for the construction of the stress profile based on analysis of breakout-type failures of the borehole wall. Considering the effective stresses in porous reservoirs, the borehole wall is a free surface due to the assumed balance between borehole mud fluid pressure and pore pressure in the vicinity of the boreholes (Zoback, 2010). This is the reason why the unconfined strength (UCS) is used for stress profile construction instead of the confined compressive strength. On the other hand, due to the technological cracking of the borehole wall while drilling, the near-borehole zone may be weakened compared to the intact reservoir rock. Fluids and pressure may penetrate within the technological micro-cracks and influence breakout failure. Following that, the effective failure conditions may become similar to those assumed in the UCST. However, they are still not the same, because the borehole wall has no technological damage associated with core relaxation, plug preparation, desiccation, and wetting of samples. Therefore, one may expect that for breakout analysis, UCS values in a wide range between 1D and 3D strength tests can be assumed.

The extremely low permeability of shale may cause preservation of pore pressure in the borehole wall below the mud pressure, which in such a scenario exerts effective stress on the borehole wall. Then, considering the origin of breakouts, the confined compressive strength under low confining pressure may be more proper than the UCS. From that point of view, higher values of UCS achieved from the CCST are more appropriate. Stress modelling conducted in two adjacent boreholes penetrating shale successions (Huffman et al., 2016) showed that the best prediction of breakout shapes was obtained by adopting Mohr-Coulomb strength criteria with UCS slightly below that determined from CCST. Our results, which gave values slightly below those from the multi-stage 3D tests, seem to be a good trade-off between the boundary options discussed.

In the common case of shale anisotropy, there also comes the question as to which values of UCS should be taken for stress analysis from breakouts, determined under vertical or horizontal directed compression? For instance, in the vertical exploration boreholes, stress estimations base on breakouts are developed predominantly under deviatoric stress in a horizontal plane. In this case, the minimum stress is defined by the mud pressure while the maximum is exerted by the enhanced far-field tectonic stress (S_{Hmax}). The situation is more complex in the case of horizontal boreholes, drilled commonly in the direction of the minimum horizontal tectonic stress (S_{hmin}), as in the case of hydraulically fractured boreholes. In that situation, initiation of breakouts can be controlled either by vertical stress (in a normal faulting stress regime) or by a horizontal one (in a strike-slip faulting stress regime). Therefore, the 12–27% UCS anisotropy that we estimated in this study can make a significant difference in stress analysis.

The weakest point of the empirical equations presented in this paper is the poor quality of correlation, especially for horizontal UCS values. However, this results from the nature of the data. Our study reveals the weaknesses of the CCST measurement configuration in terms of determining useful UCS values in the Baltic Basin. Such a poor state of the art in this aspect results from a conventional approach to the reservoir, typical for isotropic rocks, where the common practice is to perform mechanical tests in one direction, which is usually vertical (perpendicular to bedding). Such oriented samples, especially large ones, are easier to prepare along the borehole core axis. However, if the results of the UCS analysis are to be useful in further geomechanical studies, the dominant role should be assigned to the tests on horizontal samples, taken along the bedding.

CONCLUSIONS

This study includes the first compilation of a strength dataset from the Baltic Basin and the use of this for the prediction of the unconfined compressive strength (UCS), a parameter useful for stress analysis. UCS was studied in 4 boreholes in shale successions which are relatively continuous and homogeneous laterally across the basin. This allowed us to compare the results from the same lithostratigraphic formations between different boreholes.

We have compiled the results of 247 single-stage confined compressive strength tests among which 222 were performed perpendicular to bedding (vertical) and 25 parallel to bedding plane. Bringing these tests together in mechanically similar sets, we obtained 34 vertical UCS_v values and 11 horizontal UCS_h values.

Applying available Young's modulus logs from the dipole acoustic tool in vertical (E_v) and horizontal (E_h) directions, we have derived empirical equations for UCS_V and UCS_h respectively. To optimize the parameters of each formula we used the least squares method for fitting the calculated UCS values to those evaluated from the laboratory tests. For the same set of data, the linear relations between static and dynamic Young's modulus were presented, as well as the equations for UCS dependent on P-wave slowness (DTP) from log measurements, both determined in vertical and horizontal directions.

The empirical equations obtained reveal low values of the determination coefficients. The theoretical UCS values deviate from data points estimated from laboratory tests by the standard deviation in a range of (depending on the type of estimator): ±18.2–21.6 MPa for the UCS_v and 27.7–29.3 MPa for the UCS_h. Considering the high values of the UCS, these results can provide a rough estimation, more accurate for the UCS_v due to better data control.

The mean UCS values for shale formations of the B-1 borehole, calculated using our equations, gave results in the range of 85–134 MPa for UCS_V. These UCS_V values are always lower than UCS_h, by 12–27%, according to the VTI anisotropy of UCS.

These values are similar to those obtained from the multistage confined compressive strength tests on core samples from the test T-1 borehole located 15 km away from the study area. The mean laboratory-derived UCS_v values are only slightly higher than those calculated by us.

A comparison of our UCS_V values with those obtained from the unconfined compressive strength tests for samples taken in the same B-1 borehole revealed striking differences. These unconfined UCS_V values for shale formations (8–45 MPa) are several times lower than those obtained from the confined tests, both the single- and multi-stage. Such a discrepancy, also well-known from the literature, raises concerns about an option that should be taken into account for stress analysis from breakouts. Although we have no unequivocal answer to this question, our empirical equations gave moderate results, that may be useful for stress studies in the Baltic Basin.

Acknowledgements. We are grateful to the Polish Oil and Gas Co. for providing data and coordination of the ShaleMech research project as an industrial partner. Techlog software, shared by Schlumberger Information Solution to Polish Geological Institute – National Research Institute for scientific-research activities, was used in the analyses. We also thank the reviewers, P. Łukaszewski and an anonymous reviewer, for their significant contribution to improving the text of the article. The study was supported by the Polish National Centre for Research and Development, grant No. BG2/SHALEMECH/14, and the paper preparation was supported by PGI-NRI grant No. 6.2809.1701.00.0.

REFERENCES

Bonnelye, A., Schubnel, A., David, C., Henry, P., Guglielmi, Y., Gout, C., Fauchille, A.L., Dick, P., 2016. Strength anisotropy of shales deformed under uppermost crustal conditions. Journal of Geophysical Research: Solid Earth, **122**: 110–129.

Chang, C., Zoback, M.D., Khaksar, A., 2006. Empirical relations between rock strength and physical properties in sedimentary rocks. Journal of Petroleum Science and Engineering, **51**: 223–237.

Crawford, B.R., Gaillot, P.J., Alramahi, B., 2010. Petrophysical methodology for predicting compressive strength in siliciclastic "sandstone-to-shale" rocks. ARMA 65th U.S.-Canada Rock Mechanics Symposium, Salt Lake City, USA, 10–19: 27–30.

Crawford, B.R., DeDontney, N.L., Alramahi, B., Ottesen, S., 2012. Shear strength anisotropy in fine-grained rocks. ARMA 46th US Rock Mechanics/Geomechanics Symposium Chicago, USA: 12–290.

Gazaniol, D., Forsans, T., Boisson, M.J.F., Piau, J.-M., 1995. Wellbore failure mechanisms in shales: prediction and prevention. Journal of Petroleum Technology, July 1995: 589–595.

Guo, Z., Li, X-Y., Liu, C., 2014. Anisotropy parameters estimate and rock physics analysis for the Barnett Shale. Journal of Geophysics and Engineering, **11**: 065006.

Handwerger, A.D., Rivera, R.S., Keller, J., Vaughn, K., 2011. Improved petrophysical core measurements on tight shale reservoirs using retort and crushed samples. Proceedings of SPE Annual Technical Conference and Exhibition, Denver, USA.

Horsrud, P., 2001. Estimating Mechanical Properties of Shale from Empirical correlations. SPE Drilling and Completion: 68–73.

Huffman, K.A., Saffer, D.M., Dugan, B., 2016. In situ stress magnitude and rock strength in the Nankai accretionary complex: a novel approach using paired constraints from downhole data in two wells. Earth, Planets and Space, **68**: Article no. 123.

ISRM, 1983. Suggested methods for determining the strength of rock materials in triaxial compression: revised version. International Journal of Rock Mechanics and Mining Sciences and Geomechanics Abstracts, **20**: 285–290.

Jaeger, J.C., Cook, N.G., 1979. Fundamentals of Rock Mechanics. 3rd edition. Chapman and Hall, London.

Josh, M., Esteban, L., Piane, C.D., Sarout, J., Dewhurst, D.N., Clennell, M.B., 2012. Laboratory characterization of shale properties. Journal of Petroleum Science and Engineering, **88–89**: 107–124.

Khaksar, A., Taylor, P.G., Fang, Z., Kayes, T., Salazar, A., Rahman, K., 2009. Rock Strength from Core and Logs: Where We Stand and Ways to Go. SPE 121972.

King, L.V., 1912. Limiting strength of rocks under conditions of stress existing in the earth's interior. The Journal of Geology, **20**: 119–138.

Kohli, A.H., Zoback, M.D., 2013. Frictional properties of shale reservoir rocks. Journal of Geophysical Research: Solid Earth, **118**: 5109–5125.

Kovari, K., Tisa, A., Einstein, H.H., Franklin, J.A., 1983. Suggested methods for determining the strength of rock materials in triaxial compression: revised version. International Journal of Rock Mechanics and Mining Sciences, **206**: 285–290.

Mavko, G., Mukerji, T., Dvorkin, J., 2009. The Rock Physics Handbook: Tools for Seismic Analysis of Porous Media. 2nd Edition. Cambridge University Press.

Mazur, S., Mikołajczak, M., Krzywiec, P., Malinowski, M., Buffenmyer, V., Lewandowski, M., 2015. Is the Teisseyre-Tornquist Zone an ancient plate boundary of Baltica? Tectonics, **34**: 2465–2477.

Pachytel, R., Jarosiński, M., Bobek, K., 2017. Geomechanical stratification in a shale reservoir and its correlation with natural fractures: case from Pomeranian Basin (Poland). American Rock Mechanics Association Publications, Proceedings of 51st U.S. Rock Mechanics/Geomechanics Symposium: 17–77.

Poprawa, P., 2019. Geological setting and Ediacaran–Palaeozoic evolution of the western slope of the East European Craton and adjacent regions. Annales Societatis Geologorum Poloniae, **89**: 347–380.

Poprawa, P., Šliaupa, S., Stephenson, R., Lazauskiene, J., 1999. Late Vendian–Early Palaeozoic tectonic evolution of the Baltic Basin: regional tectonic implications from subsidence analysis. Tectonophysics, **314**: 219–239.

Robertson, E.C., 1955. Experimental study of the strength of rocks. GSA Bulletin, **66**: 1275–1314.

Sone, H., Zoback, M.D., 2013a. Mechanical properties of shale-gas reservoir rocks part 2: static and dynamic elastic properties and anisotropy. Geophysics, **78**: 381–392.

Sone, H., Zoback, M.D., 2013b. Mechanical properties of shale-gas reservoir rocks part 2: ductile creep, brittle strength, and their relation to the elastic modulus. Geophysics, **78**: 393–402.

Suárez-Rivera, R., Ostroff, G., Tan, K., Begnaud, B., Martin, W., Bermudez, T., 2003. Continuous rock strength measurements on core and neural network modelling result in significant improvements in log based rock strength predictions used to optimize completion design and improve prediction of sanding potential and wellbore stability. SPE 84558.

Taylor, P.G., Appleby, R.R., 2006. Integrating quantitative and qualitative rock strength data in sanding prediction studies: an application of the Schmidt hammer method. SPE/IADC 101968.

Wilczyński, P.M., Domonik, A., Łukaszewski, P., 2021. Anisotropy of strength and elastic properties of Lower Paleozoic shales from the Baltic Basin, Poland, Energies, **14**: 2995.

Wojtowicz, M., Jarosiński, M., 2019. Reconstructing the mechanical parameters of a transversely-isotropic rock based on log and incomplete core data integration. International Journal of Rock Mechanics and Mining Sciences, **115**: 111–120.

Youna, H., Tonon, F., 2010. Multi-stage triaxial test on brittle rock. International. Journal of Rock Mechanics and Mining Sciences, **47**: 678–684.

Zoback, M.D., 2010. Reservoir Geomechanics. Cambridge University Press.

Zoback, M.D., 2019. Unconventional Reservoir Geomechanics. Cambridge University Press.